10-9-2018

Evaluating the Effect of Shear Stress on Graft-To Zwitterionic Polycarboxybetaine Coating Stability Using a Flow Cell

Andrew Belanger
University of New Haven

Andre Decarmine
University of New Haven

Shaoyi Jiang
University of Washington

Keith Cook
Carnegie Mellon University

Kagya Amoako
University of New Haven, kamoako@newhaven.edu

Publisher Citation

Belanger, A., Decarmine, A., Jiang, S., Cook, K., & Amoako, K. A. (2018). Evaluating the Effect of Shear Stress on Graft-To Zwitterionic Polycarboxybetaine Coating Stability Using a Flow Cell. Langmuir. doi:10.1021/acs.langmuir.8b03078

Comments

This is the authors' submitted, preprint version of the article published in *Langmuir* by the American Chemical Society. The version of record can be found at
http://dx.doi.org/10.1021/acs.langmuir.8b03078. This article is part of the Zwitterionic Interfaces: Concepts and Emerging Applications special issue.

Evaluating the Effect of Shear Stress on Graft-to Zwitterionic PolyCarboxybetaine Coating Stability Using a Flow Cell

Kagya Amoako[*]

Andrew Belanger B.S.[a], Andre Decarmine, B.S. [b], Shaoyi Jiang Ph.D. [c], Keith Cook Ph.D. [d], Kagya A. Amoako Ph.D. [a,e]

Department of Mechanical [a] , Chemical [b] and Biomedical[e] Engineering, University of New Haven, West Haven, CT 06516, USA. Department of Chemical Engineering [c], University of Washington, Seattle WA and Carnegie Mellon University [d], Pittsburg PA

E-mail: kamoako@newhaven.edu
Dr. Kagya A. Amoako

Dept. of Mech., Ind., and Biomedical Engineering
300 Boston Post Road
West Haven, CT 06516
USA

Keywords: Shear stress, anti-fouling coatings, blood coagulation, zwitterionic polymers, fibrinogen fouling.

Abstract:

Blood-contacting devices coated with anti-clotting materials would typically fail due to clot formation after about 2 weeks of exposure to blood flow. Our overarching hypothesis for their short-term success is that the failure modes of these anti-clotting coatings are either due to 1) a slowed-pace procoagulant protein fouling, 2) their erosion due to shear stress, or 3) a combination of both. This study however partly tests the hypothesis by evaluating the effect of shear stress on coating stability. This was done by exposing DOPA-PCB-300/dopamine coated polydimethylsiloxane (PDMS) to physiological shear stresses using a recirculation system which consisted of dual chamber acrylic flow cells, tygon tubing, flow probe and meter, and perfusion pumps. The effect of shear stress induced by phosphate buffered saline flow on coating stability was characterized with differences in fibrinogen adsorption between control (coated PDMS not loaded with shear stress) and coated samples loaded with various shear stresses. Fibrinogen adsorption data showed that relative adsorption on coated PDMS that weren't exposed to shear (5.73% ± 1.97%) was significantly lower than uncoated PDMS (100%, $p < 0.001$). Furthermore, this fouling level, although lower, was not significantly different from coated PDMS membranes that were exposed to 1 *dynes/cm*^{2} (9.55% ± 0.09%, $p = 0.23$), 6 *dynes/cm*^{2} (15.92% ± 10.88%, $p = 0.14$), and 10 *dynes/cm*^{2} (21.62% ± 13.68%, $p = 0.08$). Our results show that DOPA-PCB-300/dopamine coating are stable, with minimal erosion, under shear stresses tested.

Introduction:

Large quantities of blood-contacting medical devices are used annually world-wide.[1, 2] It is estimated that more than 200 million of these devices are utilized in patients in the U.S alone. [3] They range from devices with small surface areas like catheters, vascular grafts, heart valves, cannulas, glucose, lactate sensors, and stents to those with moderate surface areas like pacemakers, artificial kidneys, and left ventricular assist devices. Then there are those with relatively larger surface areas like the artificial lungs, artificial hearts, and extracorporeal membrane oxygenation circuits.

The surfaces of these devices are made up of artificial materials that are different from endothelial cell surfaces, which interface with flowing blood.[4–6] These cells express enzymes and secrete nitric oxide that maintain blood tone.[7–10] Without these properties, blood rapidly activates into clots upon contact with artificial materials.[11, 12] For blood-contacting devices, clot formation can cause cessation of blood flow and lead to device failure[13–15]. Moreover, devices that do not fail may release clots into systemic circulation and cause embolic complications.[14, 16–18] In life support devices these clots can result in morbidity and mortality. For instance, a small bore vascular graft serving as a coronary artery may occlude from formation and cause myocardial infarction (heart attack). With artificial lungs, clotting is especially problematic as they have relatively large surface areas (1.3-2 m^2) and a period of usage lasting from several weeks to months however they typically fail after 7-14 days with accompanying hemorrhagic complications.[13–15,18] Catheters, on the other hand, have a limited lifespan and do not reliably allow repeated sampling of blood or continuous pressure monitoring in patients as their small lumen diameters make them more prone to failure by clots[19–22].

Current approaches for controlling biomaterial-induced clot formation have been largely inadequate. Commercial coatings have only shown moderate inhibition of clot formation in short-term studies[23−32] and are not sufficient to allow large decreases in systemic anticoagulation. The most successful approach to date has been to chemically immobilize heparin on blood-contacting surfaces to reduce thrombosis and lower anticoagulant administration.[33,34] Although this approach has been widely adopted, major limitations persist because the surface-bound heparin leaches, resulting in a progressive loss of anticoagulation activity.[35,36] Other hydrophilic coatings including PHISIO (Sorin) [39], Trillium (Medtronic) [40], poly-2-methoxyethyl acrylate (PMEA) polymer[41] and sulfobetaine[42] that have undergone extensive human clinical evaluation have shown no drastic non-thrombogenic benefit compared to existing heparin-coated materials.[43,44] Systemic anticoagulants hence remain the adjunctive therapy of choice although they pose an increased risk of bleeding complications. [45−47]

Important factors that affect the efficiency these coatings include their stability and coverage on devices and mechanism(s) of inhibiting coagulation. Coatings that become unstable and erode against fluid shear progressively lose their anticoagulation activity and imperfections in coating can weaken the anti-coagulation effectiveness, as procoagulant proteins can adsorb at uncoated spots. Our overall hypothesis for their short-term success is that the failure modes of these anti-clotting coatings are either due to 1) a slowed-pace procoagulant protein fouling, 2) their erosion due to shear stress, or 3) a combination of both. To test our hypothesis, a relatively new coating material that has shown ultra-low auto-adsorption of pro-coagulant proteins, polycarboxybetaine,[48-50] was used to study the effect of shear stress on coating stability.

PDMS coated with DOPA-PCB-300/dopamine were exposed to shear stresses similar to those found in the vena cava, large veins, and conduit arteries.[51]

Methods

Flow Cell and Flow Recirculation Circuit Design: The dual chamber flow cell and recirculation system design is shown in **Figure 1**. It consists of an acrylic (Custom Creative Plastics, FL) flow cell that was designed using Autodesk inventor (San Rafael, CA), a 3/16" I.D. and 5/16" O.D. tygon tubing circuit (Fisher Scientific, MA), a pump (Stöckert Shirley multiflow roller blood perfusion pump, SOMA Tech. Bloomfield, CT), Transonic flow probe and meter (Transonic Inc. Cambridge MA) and Leuer lock priming

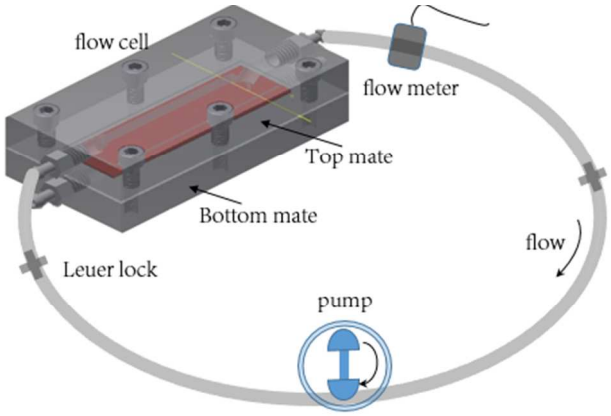

Figure 1. Recirculation circuit for testing flow effects on the stability of surface-modified samples. Circuit consist of an acrylic dual chamber flow cell in which samples are placed, a flow meter to measure volumetric flow rates, a perfusion pump to circulate fluid through Tygon tubing.

ports. The flow cell assembly of top and bottom mates measures Length = 11.43 *cm*, width = 5.87 *cm*, height = 1.60 *cm*. and are attached to a recirculation circuit using polycarbonate connectors (Qosina, NY)**.** The flow cell chamber measures a 1 cm x 6.35 *cm* x 0.5 *cm* with a hydraulic diameter = 0.67 *cm*, entrance area = 0.37 cm^2. Test samples (surface modified or unmodified), represented by the rectangular piece inside the flow cell, are first affixed onto the bottom mate's flow chamber already lined with an

adhesive nitrile sponge rubber gasket (Grainger.com, Lake Forest, IL) followed by the application of a gasket-lined top mate and compression of top and bottom mates with screws.

Leak Testing, Pump Calibration, and Shear Stress Characterization: To ensure no leakages during application of flows over samples, a leak test was performed under experimental test conditions. A PDMS sample measuring 8.89 *cm* x 2.54 *cm* was inserted into the recirculation circuit and primed with 35mL of phosphate buffered saline (PBS) ensuring that no air bubbles were present in the circuit before flow initiation. Recirculation was maintained for 8 hours at low flow (30 *mL/min*) and high flow (1500 *mL/min*). Since the blood perfusion pumps used in this experiment are roller pumps that display only digital revolutions per minute (rpm) readouts, it was necessary to determine their flow rates as a function of rpms. First, their tubing occlusion were set at the recommended clinical pump occlusion setting where a 100cm fluid column drops 25cm/min[52-53]. At this occlusion setting, a calibration curve of rpm versus flow rates was generated by pumping of PBS from a reservoir to an empty container. Rpms were set at 50, 100, and 150 and the pumped volume and pumping time recorded. An rpm to flow rate calibration curve was generated for each pump so that a relation of wall shear stress as a function average flow velocity (flow rate/cross sectional area), fluid dynamic viscosity, and hydraulic diameter of flow chamber could be developed.

Wall shear stress was calculated as

$$\boldsymbol{\tau_o = f(\rho \times V_{avg}{}^2)}, \text{ where}$$

$\boldsymbol{\tau_o}$ Wall shear stress (N/m^2),

f Darcy-Wiesbach friction factor for the acrylic chamber surface is $f = \frac{64}{\mathrm{Re}}$ since flow is laminar,

Re Reynolds number,

ρ Density of fluid (kg/m^3),

$V_{avg} = \frac{flow\ \mathrm{rate}}{\mathrm{flow\ chamber\ x-section\ area}}$ (m/s).

The entrance length, L_e, was expressed in terms of Reynolds number and hydraulic diameter as $L_e = 0.06 \times Re \times D_h$ where D_h is the hydraulic diameter of the flow chamber given as $\frac{4 \times A_c}{2(b+h)}$, where A_c is cross sectional area and ***b*** and ***h*** are width and height of the chamber entrance. The entrance length was calculated to be 0.04 *cm* using D_h = 0.67 *cm* and $Re \sim 1$.

Coating PDMS with DOPA-pCB-300/dopamine and Coating Stability

Characterization: PDMS membrane (NuSil Tech. CA) measuring 8.89 *cm* x 2.54 *cm* were casted via two-part polymerization process. Cured PDMS membranes were coated with DOPApCB-300 using a dip-coating process previously described.[50] Briefly, PDMS was immersed in TRIS buffer (pH 8.5) containing dissolved 2.8 *mg/mL* DOPA-PCB-300/dopamine mixture at a ratio of 1:40. Buffer with PDMS was gently agitated for 2hrs. A schematic of the coating process is presented in **Figure 2**.

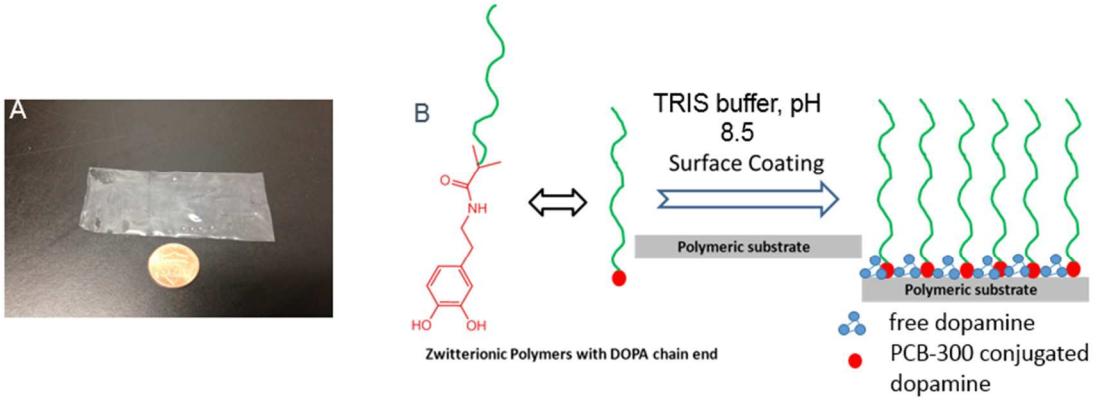

Figure 2. Grafting of DOPA-pCB-300/dopamine mixed coatings at a ratio of 1 DOPA-pCB-300 :40 dopamine in TRIS buffer (pH 8.5) at 2h coating time on PDMS. **A)** Shows PDMS substrate and **B)** shows DOPA-PCB-300 attachment onto PDMS.

Uncoated (N=5 samples at stagnant, no flow) and coated membranes (N=5 samples/test condition) were inserted into flow cells (**Figure 3D**) and the circuits were primed with phosphate buffered saline, pH= 7, (Sigma Aldrich, MO). Flows were initiated at 60 *mL/min*, 150 *mL/min* and 230 *mL/min* and recirculated through the flow cells for 8 hours. For each run, a set of four test conditions (coated PDMS with 0, 1, 6, and 10 *dynes/cm*^{2}) were evaluated followed by test runs for uncoated no flow samples. These flows yield physiologically relevant shear stress of 1 *dyne/cm*^{2}, 6 *dynes/cm*^{2} and 10 *dynes/cm*^{2}. The membranes were carefully removed after recirculation and stored in PBS. Three 1 *cm* x 1 *cm* pieces from each sample were sectioned and prepared for standard fibrinogen adsorption ELISA as previously described.[50] The circuits were soaked in 10% bleach overnight, rinsed with DI water and dried with pressurized nitrogen between test runs.

Fibrinogen Adsorption Assay: Briefly, the 1 *cm* x 1*cm* squares were placed into a 24-well plate and incubated in 1 *mL* of 1 *mg/mL* fibrinogen for 90 minutes at room temperature. The disks are then washed five times with PBS and incubated with 1mL of 1 mg/mL BSA (Sigma Aldrich) for 90 minutes at room temperature. The samples were again washed five times with PBS. Next, the samples were transferred into new wells and incubated in 1:1000 dilution of HRP (Sigma Aldrich) anti fibrinogen in PBS for 30 minutes, followed by another wash in PBS. The samples were then transferred to a new set of wells. The solution is then incubated in 500 uL of 1 *mg/mL* OPD (Sigma Aldrich) in 0.1 M citrate-phosphate buffer containing 0.03% hydrogen peroxide. This reaction was then quenched after 30 minutes by the addition of 500 *uL* of 1N HCL (Sigma Aldrich). The supernatant was then removed from each sample and transferred into

cuvettes. The absorbance of each supernatant was then measured at 492 *nm* using UV-vis spectrophotometer (Beckman Coulter, CT). It was expected that uncoated PDMS samples would have higher absorption of fibrinogen and thus higher UV-vis absorbance levels. The effect of coating erosion on biocompatibility was determined as the percent increase in fibrinogen adsorption compared to appropriate DOPAPCB-300/dopamine coated PDMS controls. Less than 10% increment was considered highly stable, between 10 – 30% increase was considered stable and 30% or greater was considered unstable.

Statistical Analyses: A single factor ANOVA (SPSS, Chicago IL) was run to determine statistical differences between controls (uncoated PDMS, and DOPApCB-300/dopamine coated PDMS with no flow) and coated PDMS exposed to 1 *dynes/cm*^{2}, 6 *dynes/cm*^{2} and 10 *dynes/cm*^{2} shear stresses. A $p < 0.05$ was regarded as significant.

Results and Discussion

The exploded view of the flow cell design showing top and bottom mates, cell chamber, gasket channel circuit connectors are shown in **Figure 3A** and **Figures 3B and 3C** are the flow cell and recirculation circuit prototypes. There were also no observable leaks or air bubbles in the circuit during all runs. The 5 *mL* syringe in Figure 3C was used to

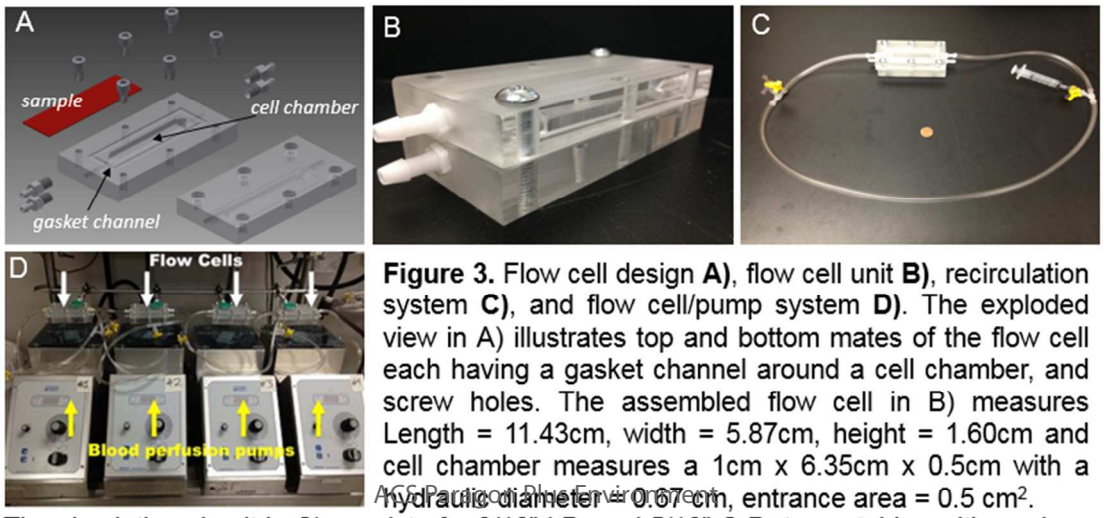

Figure 3. Flow cell design **A)**, flow cell unit **B)**, recirculation system **C)**, and flow cell/pump system **D)**. The exploded view in A) illustrates top and bottom mates of the flow cell each having a gasket channel around a cell chamber, and screw holes. The assembled flow cell in B) measures Length = 11.43cm, width = 5.87cm, height = 1.60cm and cell chamber measures a 1cm x 6.35cm x 0.5cm with a hydraulic diameter = 0.67 cm, entrance area = 0.5 cm^2. The circulation circuit in C) consist of a 3/16" I.D. and 5/16" O.D. tygon tubing with a prime volume of 35mL and D) shows four flow cell/pump units for multi flow conditions testing.

prime and extract trapped bubbles during priming.

As presented in **Figure 4**, the rpm to flow rate calibration of pumps showed linear relationships between the two variables although there were some pump-pump variation indicated by the rpm-to-pump data fitting equations. The coefficient of determination, R^2, for pumps 1, 2, 3 and 4 were 0.99, 1, 0.99, and 0.99 respectively.

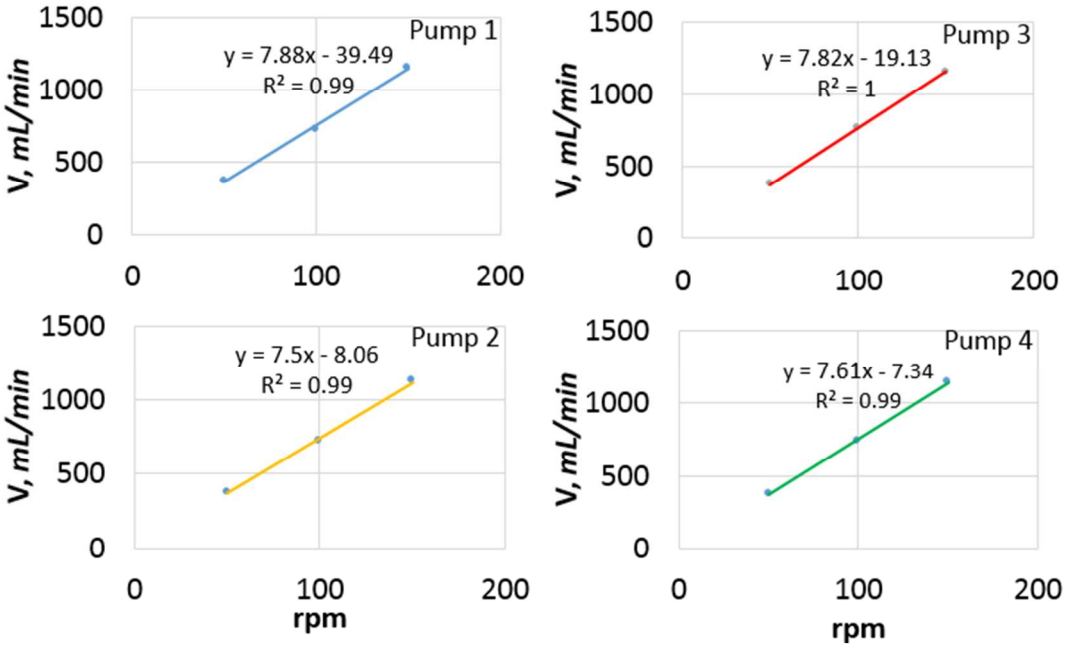

Figure 4. Revolution per minute (rpm) to volumetric flow (mL/min) calibration curves of four perfusion pumps 1,2,3, and 4 that were used to recirculate phosphate buffered saline over DOPA-PCB-300/dopamine coated samples.

Each pump's rpm-to-flow rate output provided guidance to obtain desired flow rates. Knowing the flow rates and obtaining the average flow velocity by dividing flow rates by the cross-sectional area of the cell chamber, sample or wall shear stress could be calculated using the τ_o equation from the methods section. **Figure 5** shows the wall shear stress on the primary axis as a function of flow rate and Reynolds number on the secondary axis as a function of flow rate. After fitting calculated shear stress to flow rate

date, it was determined that the calculated wall shear,$\boldsymbol{\tau_o}$, increased with flow rate according to $\boldsymbol{\tau_o = 0.02\left(\frac{dynes \times min}{cm^2 \times mL}\right) \times V\left(\frac{mL}{min}\right) - 4E - 15\left(\frac{dynes}{cm^2}\right)}$. In the shear stress calculation, the Darcy-Wiesbach friction factor depended on only the Reynolds number since the pre-calculated Reynolds number was < 2300. Shown also in **Figure 5**, we see that the Reynolds numbers calculated from the experimental flow rates and fluid

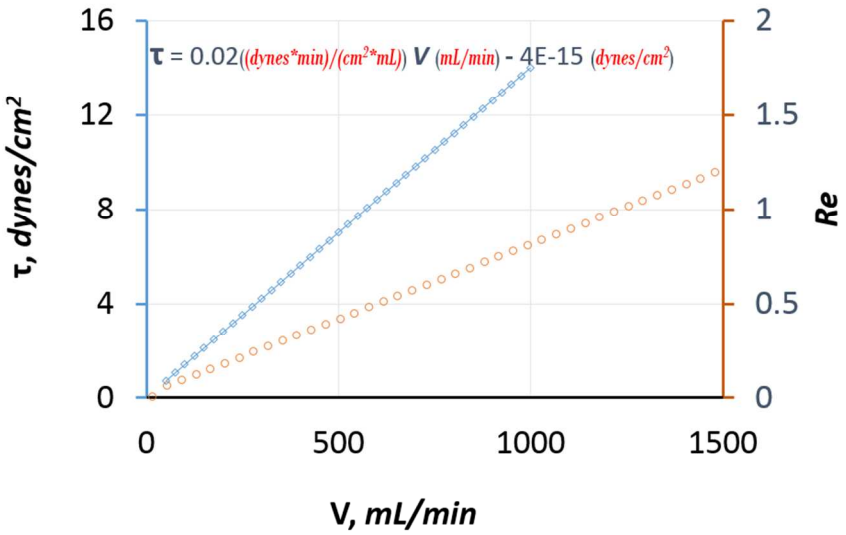

Figure 5. Physiologically relevant shear stresses (1 dynes/cm^2, 6 dynes/cm^2, and 10 dynes/cm^2) induced by laminar (Reynolds numbers 0.25 to 2) volumetric flows over samples placed inside flow cells.

properties were low and ranged from 0.25 – 1.25.

Although the Reynolds numbers were low, a comparison of flow entrance length to cell chamber length was made to determine whether turbulent flow effects typical at flow entrances were dominant over entire length. The calculated entrance length, $\boldsymbol{L_e}$, was 0.04 *cm* and compared to the cell chamber length = 6.35 *cm,* which is a two orders of magnitude bigger indicating that almost the entire sample surface and therefore the cell chambers saw fully developed laminar flows. Because the wall shear stress,$\boldsymbol{\tau_o}$, remains constant along the flow direction in the fully developed regions of both turbulent

or laminar flows, it was also deduced that almost all of the sample surface area saw constant non-zero shear stresses during flow. However, in the entrance region, τ_o isn't constant but rather starts out larger before decreasing to a constant stress in the fully developed region for any given flow rate. Therefore flow-induced erosion of DOPA-PCB-300/dopamine may be possible and perhaps higher in the entrance length region than what may occur in the fully developed flow region. It should be noted that the scenario described above only reflects shear stress dynamics in a single fluid flow pass while the continued interaction between the velocity profile and the samples from multiple passes may further influence coating stability. Subsequent passes may cause repeated interferences of the fully developed flow profile at the tubing/flow cell connection and lead to repeated and transient increases in shear stress in the entrance length region which may further influence the stability of the coating especially in high shear stress test conditions. This theory is supported by the fibrinogen adsorption data from coated samples that were exposed to shear stresses. Fibrinogen fouling before flows on DOPA-PCB-300/dopamine coated PDMS (5.73 ± 1.97%) was significantly lower than uncoated PDMS (100%, $p < 0.001$) as shown in **Figure 6**. The data shows that fibrinogen fouling on coated samples increase with increasing shear stress although to levels not significantly different from control (coated samples not loaded with shear stress). In addition, fouling on coated PDMS with zero shear stress, although lower, was not significantly different from coated samples that were exposed to 1

dynes/cm^2 (9.55% ± 0.09%, p = 0.23), 6 dynes/cm^2 (15.92% ± 10.88%, p = 0.14), and

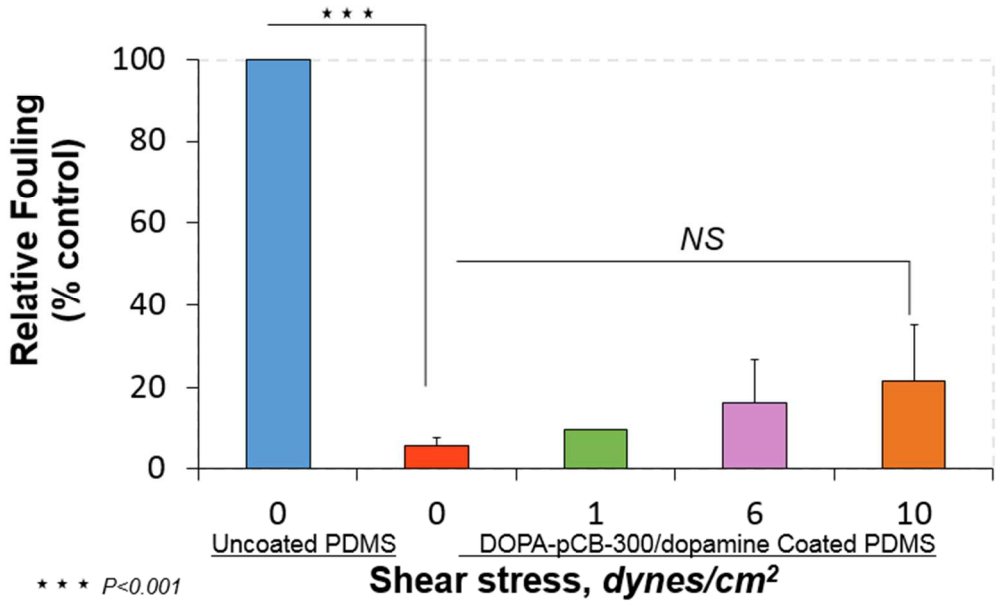

Figure 6. Fibrinogen adsorption levels on coated PDMS membranes exposed to different shear stresses

10 *dynes/cm*^{2} (21.62% ± 13.68%, p = 0.08). Our findings show that DOPApCB-300/dopamine coating were stable under the test conditions and only minimal coating erosion was observed. Compared to the coated PDMS no shear stress case, coated surfaces that were exposed to 1, 6, and 10 *dynes/cm*^{2} of shear stress, adsorbed 3.83%, 10.20%, and 15.90% more fibrinogen respectively. It should be noted that the experiment was conducted at room temperature and with pH 7 PBS which are different from in-vivo conditions where the surface will interact with blood flow at a higher temperature. The study design used here however allows for a direct measurement of nonspecific protein adsorption on coated model surfaces after they have been exposed to flow, allowing for quantification of the stability of any non-fouling coating or surface immobilized enzymes against shear stress. Contamination of sample surfaces with biological material from stability testing with whole blood and perhaps plasma, on the

other hand, could lead to unreliable coating stability data using this approach. Non-specific protein fouling on coatings exposed to blood or plasma flow shear stress would be simply difficult to evaluate.

Conclusion

In this study, the stability of a low-fouling DOPA-PCB-300/dopamine coating against various flow-induced shear stresses was measured. It was found that instability, as measured by percent increase in fibrinogen fouling between shear treated and no shear samples, increases with shear stress. To conduct the experiment, flow cells were fabricated and characterized for flows that yield different shear stresses (1 *dynes/cm*^{2}, 6 *dynes/cm*^{2}, and 10 *dynes/cm*^{2}). The surfaces of PDMS membranes were then coated with low fouling DOPA-PCB-300/dopamine followed by testing of the coating's stability against those shear stresses by placing the coated PDMS samples inside the flow cells and recirculating PBS over the samples at given flow rates for 8 hrs. Fibrinogen fouling between shear stress and no shear stress coated samples were compared to determine differences. Less than 10% increment was considered highly stable, between 10 – 30% increase was considered stable and 30% or greater was considered unstable. Compared to the coated PDMS with no shear stress case, coated surfaces that were exposed to 1, 6, and 10 *dynes/cm*^{2} of shear stress, respectively adsorbed 3.83%, 10.20%, and 15.90% more fibrinogen. Our results therefore show that DOPApCB-300/dopamine coating were stable and only minimal coating erosion was observed. As newer and more robust anticlotting coatings get developed, this simple and easy-to-use in-vitro flow cell system provides an appropriate pre-in vivo screening tool for determining coating stability under flow before conducting animal testing. The flow

system can be used to evaluate many coatings and surface modifications in biomaterials and blood-contacting devices. Other biomarkers for blood coagulation can be studied with this flow cell as well as evaluating the effects of pH and temperature. . The gas transfer properties of polymeric materials and interrogation of human cells and microorganisms such as bacteria and viruses with polymer permeable agents like nitric oxide could also be studied taking advantage of the dual chamber design of the flow cell. The results here suggest that coating erosion play a role in reducing the effectiveness of anti-fouling coatings used on blood-contacting medical devices.

References

1. Ratner BD. The blood compatibility catastrophe. J Biomed Mater Res **1993**; 27: 2837
2. Hanson SR, Ratner BD. Evaluation of blood-materials interactions-Biomaterials science: an introduction to materials in medicine. San Diego, **2004**; 36778
3. Ratner DB. The catastrophe revisited: Blood compatibility in the 21st century. Biomaterials **2007**; 28: 5144
4. Stuehr DJ, Kwon NS, Nathan CF, Griffith OW, Feldman PL, Wisean J. N omega-hydroxy-L-arginine is an intermediate in the biosynthesis of nitric oxide from L-arginine. J Biol Chem **1991**; 266: 6259
5. Marlett MA. Nitric oxide: biosynthesis and biological significance. Trends Biochem Sci **1989**; 14:488
6. Kushwaha M, Anderson JM, Jun HW. A nitric oxide releasing, self-assembled peptide amphiphile matrix that mimics native endothelium for coating implantable cardiovascular devices. Biomaterials **2010**; 31:1502
7. Gnarro IJ. Biosynthesis and metabolism of endothelium-derived nitric oxide. Annual Rev Pharmacol Toxicol **1990**; 30:535
8. Rapoport RM, Draznin MB, Murad F. Endothelium-dependent relaxation in rat aorta may be mediated through cyclic GMP-depedent protein phospharylation. Nature **1983**, 306:174
9. Palmer RM, Ferrige AG, Moncada S. Nitric oxide release accounts for the biological activity of endothelium- derived relaxing factor. Nature **1987**; 337:524
10. Xu WM, Liu LZ. Nitric oxide: from a mysterious labile factor to the molecule of the Nobel Prize. Recent progress in nitric oxide research. Cell Res. **1998**; 8(4): 251
11. Colman RW, Hirsh J, Marder VJ, Clowes AW, and George NJ. (2001) Hemostasis and Thrombosis: Basic Principles & clinical Practice, 4th Edition: Lippincott Williams & Wilkins, Philadelphia, PA, USA.

12. Major TC, Brant DO, Burney CP, Amoako KA, Annich GM, Meyerhoff ME, Handa H, and Bartlett RH. The hemocompatibility of a nitric oxide generating polymer that catalyzes S-nitrosothiol decomposition in an extracorporeal circulation model. Biomaterials **2011**; 32: 5957
13. Cook KE, Perlman CE, Backer CL, Mavroudis C and Mockros LF. Hemodynamic and gas transfer properties of a compliant thoracic artificial lung. ASAIO Journal **2005**; 51:404
14. Bartlett RH. Extracorporeal life support registry report 1995. ASAIO Journal **1997**; 43:104
15. Sato H, Griffith GW, Hall CM, Toomasian JM, Hirschl RB, Bartlett RH and Cook KE. Seven-Day Artificial Lung Testing in an In-Parallel Configuration, Ann Thorac Surg **2007**; 84:988
16. Amoako KA, Cook KE. Anticoagulant properties of copper-doped nitric oxide-generating silicone. ASAIO Journal **2011**; 57:539
17. Murphy J, C. Savage, S. Alpard, D. Deyo, et al. Low-dose versus high-dose heparinization during arteriovenous carbon dioxide removal Perfusion. **2001**; 16(6); 460
18. Zhang Z, Zhang M, Chen S, Horbert TH, Ratner BD and Jiang S. Blood compatibility of surfaces with superlow protein adsorption Biomaterials **2008**; 29:4285
19. Bass J, Halton J, Drouet Y, Ni A, Barrowman N. Central venous catheter database: an important issue in quality assurance. Journal of Pediatric Surgery **2011**; 46, 942
20. Dillon PA, Foglia RP. Complication associated with an implantable vascular access device. J Pediatr Surg **2006**;41:1582-7
21. Male C, Chait P, Andrew M, et al. Central venous linerelated thrombosis in children: association with central venous line location and insertion technique. Blood **2003**; 101:4273
22. Journeycake JM and Buchanan GR. Catheter-related deep venous thrombosis and other catheter complications in children with cancer. J Clin Oncol **2005**; 24:4575
23. Winthrop AL and Wesson DE. Urokinase in the Treatment of Occluded Central Venous Catheters in Children. Journal of Pediatric Surgery **1984**; 19(5): 536
24. Anton N, Cox PN, Massicotte MP, Chait P, Yasui L, Dinyari PM, et al. Heparin-bonded central venous catheters do not reduce thrombosis in infants with congenital heart disease: A blinded randomized, con- trolled trial. Pediatrics **2009**;123: 453
25. Masaru Tanaka, Tadahiro Motomura, Miho Kawada, Takao Anzai, Yuu Ka- sori, Toshifumi Shiroya, Kenichi Shimura, Makoto Onishi, Akira Mochizuki. Blood compatible aspects of poly(2-methoxyethylacrylate) (PMEA)- relationship between protein adsorption and platelet adhesion on PMEA surface Biomaterials **2000**; 21:1471
26. M. Kocakulak, C. Kocum, R. Saber, H. Ayhan, S. Gunaydin, T. Sari and Y. Zorlutuna, N. Bingol. Inves- tigation of blood compatibility of PMEA coated extracorporeal circuits. Journal of Bioactive and compatible polymers, **2002**; 17:343

27. Larson DF, Arzouman D, Kleinert L, Patula V and Williams S. Comparison of Sarns 3M heparin bonded to Duraflo II and control circuits in a porcine model: macro- and microanalysis of thrombi accumulation in circuit arterial filters. Perfusion **2000**; 15:13
28. Babapulle MN, Eisenberg MJ. Coated stents for the prevention of restenosis: Part I. Circulation **2002**; 106:2734
29. Yoshinari Niimi, Fumito Ichinose, Yoshiki Ishiguro, Katsuo Terui, Shoichi Uezono, Shigeho Morita,and Shingo Yamane. The Effects of Heparin Coating of Oxygenator Fibers on Platelet Adhesion and Protein Adsorption. Anesth Analg **1999**; 89:573
30. Masaru Tanaka, Tadahiro Motomura, Miho Kawada, Takao Anzai, Yuu Kasori, Toshifumi Shiroya, Kenichi Shimura, Makoto Onishi, Akira Mochizuki. Blood compatible aspects of poly(2-methoxyethylacrylate) (PMEA)- relationship between protein adsorption and platelet adhesion on PMEA surface Biomaterials 21 **2000**;1471
31. Jeanette M van den Goor, Willem van Oeveren, Peter M Rutten, Jan G Tijssen and Len Eijsman. Adhesion of thrombotic components to the surface of a clinically used oxygenator is not affected by Trillium coating Perfusion **2006**; 21: 165
32. Serdar Gunaydin. Clinical significance of coated extracorporeal circuits: a review of novel technologies. Perfusion **2004**; 19: S33-S41
33. Peppas, N. & Langer, R. New challenges in biomaterials. *Science* **1994**; 263, 1715
34. Larm, O., Larsson, R. & Olsson, P. A new non-thrombogenic surface prepared by selective covalent binging of heparin via a modified reducing terminal residue. *Biomater. Med. Devices Artif. Organs* **1983**; 11, 161
35. Conn, G. et al. Is there an alternative to systemic anticoagulation, as related to interventional biomedical devices? Expert Rev. Med. Devices **2006**; 3, 245.
36. Bannan, S. et al. Low heparinization with heparin-bonded bypass circuits: is it a safe strategy? Ann. Thorac. Surg. **1997**; 63, 663
37. Lobato, R.L. et al. Anticoagulation management during cardiopulmonary bypass: A survey of 54 North American institutions. J. Thorac. Cardiovasc. Surg. **2010**; 139, 1665
38. Shen, J.I., Mitani, A.A., Chang, T.I. & Winkelmayer, W.C. Use and safety of heparin-free maintenance hemodialysis in the USA. Nephrol. Dial. Transplant. **2013**; 28, 1589
39. Thiara, A.S. et al. Comparable biocompatibility of Phisio- and Bioline-coated cardiopulmonary bypass circuits indicated by the inflammatory response. Perfusion **2010**; 25, 9
40. Palanzo, D.A. et al. Effect of Carmeda® BioActive Surface coating versus Trillium™ Biopassive Surface coating of the oxygenator on circulating platelet count drop during cardiopulmonary bypass. Perfusion **2001**; 16, 279
41. Suhara, H. et al. Efficacy of a new coating material, PMEA, for cardiopulmonary bypass circuits in a porcine model. Ann. Thorac. Surg. **2001**; 71, 1603

42. Smith, R.S. et al. Vascular catheters with a nonleaching poly-sulfobetaine surface modification reduce thrombus formation and microbial attachment. Sci. Transl. Med. **2012**; 4, 153
43. Kutay, V. et al. Biocompatibility of heparin-coated cardiopulmonary bypass circuits in coronary patients with left ventricular dysfunction is superior to PMEA-coated circuits. J. Card. Surg. **2006**; 21, 572
44. Reser, D. et al. Retrospective analysis of outcome data with regards to the use of Phisio®-, Bioline®- or Softline®-coated cardiopulmonary bypass circuits in cardiac surgery. Perfusion **2012**; 27, 530
45. LaBan MM, Whitmore CE, Taylor RS. Bilateral adrenal hemorrhage after anticoagulation prophylaxis for bilateral knee arthroplasty. Am J Phys Med Rehabil **2003**; 82:418
46. Campbell BT, Braun T, Schumacher R, Bartlett RH, Hirschl RB. Impact of ECMO on neonatal mortality in Michigan (1980-1999). J Ped Surg **2003**; 38(3): 290
47. Bartlett RH, Roloff DW, Custer JR, Younger JG, Hirschl RB. Extracorporeal Life Support. The University of Michigan experience. JAMA **2000**; 283(7): 904
48. Amoako, KA. Nitric oxide therapies for local inhibition of platelets' activation on blood-contacting surfaces. Diss. The University of Michigan, 2011
49. S.Jiang and Z.Q.Cao, Ultralow Fouling, Functionalizable, and Hydrolyzable Zwitterionic Materials and Their Derivatives for Biological Applications, Advanced Materials **2010**; 22: 920
50. Sundaram, H. S., Han, X., Nowinski, A. K., Brault, N. D., Li, Y., Ella-Menye, Jean-Rene, Amoako, K. A., Cook, K. E., Marek, P., Senecal, K., Jiang, S. (**2014**). Achieving One- Step Surface Coating of Highly Hydrophilic Poly(Carboxybetaine Methacrylate) Polymers on Hydrophobic and Hydrophilic Surfaces. Adv. Mater. Interfaces, doi:12. 10.1002/admi.201400071
51. Papaioannou, Christodoulos stefanadis. "Vascular Wall Shear Stress: Basic Principles and Methods" Hellenic J Cardiol **2005**; 46: 9
52. L B Mongero, J R Beck, T W Orr, R M Kroslowitz, K Lee-Sensiba and M C Oz Clinical evaluation of setting pump occlusion by the dynamic method: effect on flow. *Perfusion* **1998** 13;5: 360
53. Sarns™, 8000 Modular Perfusion System, operator's manual, roller pump software version 2.3L. **1993**; 2.1-2.14